Society of Petroleum Engineers

SPE-194269-MS

An Advanced Technique for Simultaneous in Situ Inspection of Multiple Metallic Tubulars

Yanxiang Yu, William Redfield, Nicholas Boggs, Kuang Qin, Marvin Rourke, and Jeff Olson, GOWell International, LLC; Mosunmola Ejike, Fluor Federal Petroleum Operations

This paper was prepared for presentation at the SPE/ICoTA Well Intervention Conference and Exhibition held in The Woodlands, TX, USA, 26-27 March 2019.

Abstract

A new pulsed eddy current (PEC) - electromagnetic (EM) based tool called the enhanced Pipe-thickness Detection Tool (ePDT) has been introduced for multiple pipes' corrosion inspection. The tool can measure the metal wall thickness of five concentric pipes with the maximum outer diameter (OD) up to 26". This capability and ePDT's unique configuration provide the most advanced downhole solution for tubular evaluations of production, injector and gas/oil storage wells. The ePDT features a 2" (51mm) OD with ratings of 350°*F* (175°*C)* and 20,000 psi (138Mpa).

The innovative sensor of ePDT incorporates: (1) A fractal transmitter (TX) coil array that improves the tool's performances with enhanced signal-to-noise ratio (SNR) covering a wide signal dynamic range, and adaptability for various logging speeds and spatial resolutions for varying pipes; (2) A synthetic aperture of the receiver (RX) coil array for noise compensation from extraneous tool motion; (3) A wide-spatial aperture RX coil array which when combined with (1) and (2) allows for compressing the inner pipe remnant magnetization interferences without sacrificing spatial resolution; (4) A "shallow" measuring transducer to detect EM properties for logging data corrections.

The results from lab tests and field trials combined with simulation indicate that the ePDT can quantitatively measure 5 pipes from 2-7/8" as the smallest tubing to the maximum outer casing with the OD of 26". In addition, the logging speed can be significantly increased compared to previous generation tools.

Introduction

Well Integrity (WI) monitoring is gaining more attention due to aging hydrocarbon production and storage wells along with new production and storage wells exposed to elevated concentrations of corrosive fluids. These factors have impacted well performance, safety, environmental concerns and stricter regulations. Early and periodic monitoring of tubulars corrosion and other defects can cost-effectively reduce the risks of serious leaks or well failures.

Multiple techniques for detecting and quantifying an array of corrosion and various other wellbore defects are currently available. For example, multi-finger caliper and video camera imager can examine the inner surface of tubing; ultrasonic tool and magnetic flux leakage tools can provide accurate assessment

of both inner and outer surface for the first string. Historically, the continuous sinusoidal-signal-based Far-Field Eddy Current (FFEC) technologies have been developed and deployed for multiple concentric pipe average thickness measurements. However, FFEC is adversely influenced by the strong interference of the direct excitation signal transmission coupling and EM skin effect, this reduces the pipe response due to a decreasing SNR that does not allow quantitative evaluation of more than two concentric pipes. Many efforts have been made from the technology providers to overcome the problems (Martin, et al. 2017, Omar, et al. 2018). Examples include:

1. Measuring at multiple frequencies and utilizing multiple TX-RX pairs to separate pipes' responses;
2. Increasing excitation signal level to boost SNR;
3. Reducing the frequencies to measure more and larger pipes;
4. Separating and spacing the transmitter coils and receiver coils to reduce direct coupling and interference from inner pipes.

These improvements however create new challenges for downhole logging operations, which include:

1. Increasing tool complexity and error propagation in combined data processing due to the measurements from multiple TX-RX pairs;
2. Low resolution due to the large TX-RX spacing/aperture;
3. Strong direct coupling interference from high excitation signals;
4. Very slow logging speed for the phase measurement due to very low frequency signal;
5. Non-linear TX-RX aperture to generate ghost effects due to the large TX-RX spacing;
6. Aliasing from under sampling with the combination of logging speed, low logging rate with low frequency, and non-linear TX-RX transducer aperture.

In contrast, the PEC excited EM signal that contains wide-band frequency components from kilo Hertz to sub Hertz range. The low frequency EM signals effectively penetrate concentric metal pipes. The induced PEC on each tubular has different initial amplitude and decay rate due to combination of its OD, thickness, and EM parameters. After excitation, magnetic field changes triggered by a combination of mutual inductive interactions among the pipes, eddy current diffusion and damping are picked up by the receiving coil during the acquisition window. Researches and field applications have proven that PEC method is more reliable for multiple pipes' average thickness detection. In our previously published papers (Rourke, M., et al, 2014), three pipes with up to 17" OD can be detected by the MTD generation tools. However, the combination of high signal dynamic range, inadequate SNR, extraneous tool motion, and troublesome interference of pipe magnetization. It has proven difficult for MTD to reliably quantify the outer pipes' thicknesses in the presence of more than three concentric tubulars or at OD larger than 17".

In this paper, we will present a new generation of PEC tool, the ePDT. It has been designed to quantify the average thickness of up to five concentric pipes with a maximum OD up to 26". The tool has a segmented fractal array transducer in different spatial apertures to cover measurements for different pipes: the smallest TX-S accurately measures EM parameters from smallest tubular for data correction; the medium TX-M provides an optimal balance between log resolution and SNR for each pipe measurements; and the largest TX-L generates high SNR for larger outer pipe measurements. The synthetic aperture design of the RX coil array incorporated with the fractal TXs can help to reduce the extraneous tool motion and tubing remnant magnetization noise. By applying a hybrid fast inversion method, the thickness of each pipe could be calculated. The design concepts, tool specifications, and measurement integrity of ePDT have been verified and validated through simulations, lab tests, and field loggings. The results and conclusion will be illustrated and discussed in the paper.

The following sections will discuss the ePDT tool configuration, tool modeling, processing algorithm, lab verification study, and field log cases. The field log data collected so far demonstrates that ePDT can

measure the thickness of a third pipe with OD of 20". Furthermore, the unambiguous signal of a fourth casing with an OD of 30" has been successfully detected, while due to inadequate SNR, the quantitative analysis for the pipe thickness is not provided. Finally, tests of data repeatability and validity at various logging speeds are studied and presented.

ePDT Tool Description

ePDT tool contains two modules: Sensors Section with TX coil arrays and RX coil arrays, and Electronics Section with various units for power supply, excitation driver, data acquisition, data pre-processing, data communication, and tool control. The two sections are connected through the field joint, reference Fig. 1 below.

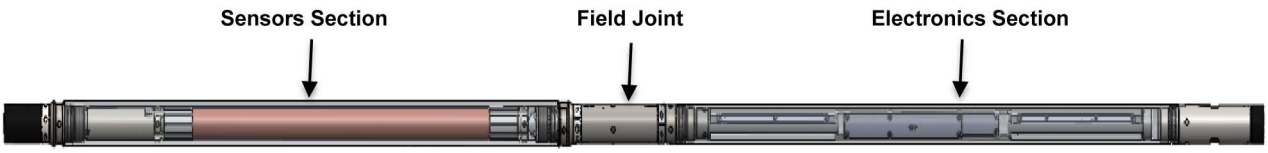

Figure 1—ePDT mechanical structure

For ePDT logging operations, the complete logging system requires surface panel, downhole telemetry/ power module, and centralizers as shown below in Fig. 2.

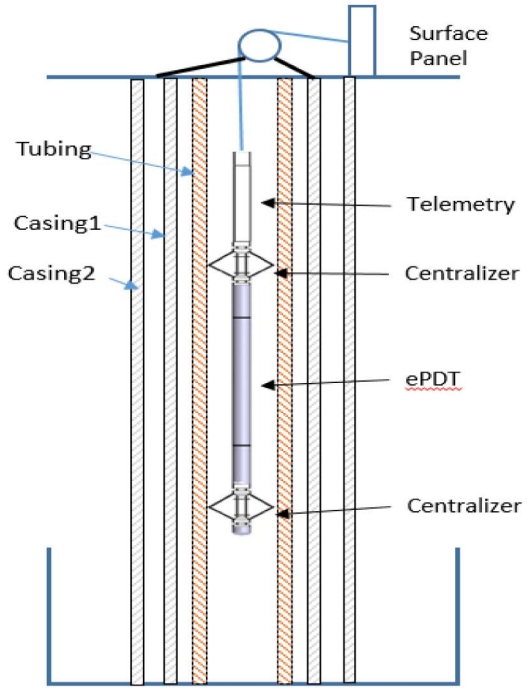

Figure 2—ePDT logging system

During logging, ePDT excites current signal through a TX coil array, to magnetically charge the metal pipes. Once the magnetic field B_0 is stabilized, ePDT rapidly halts the charging current in order to induced high initial EC trigged by dB_0/dt in the target. Concurrently, ePDT starts acquiring the corresponding time transient signal from the RX coil array as dB_{EC}/dt, which reflects the EC diffusing and damping, the time variant signal is associated with pipe properties and geometries that indicate the pipe thickness changes due to corrosion or other defects, as illustrated in Fig. 3.

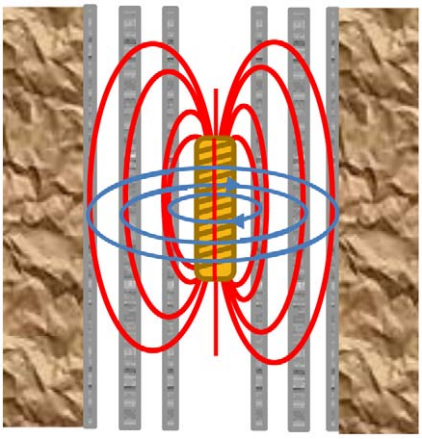

Figure 3a—Physical model of PEC sensor, red lines indicate the induced magnetic flux, and blue lines illustrate eddy current flow in the metallic pipes

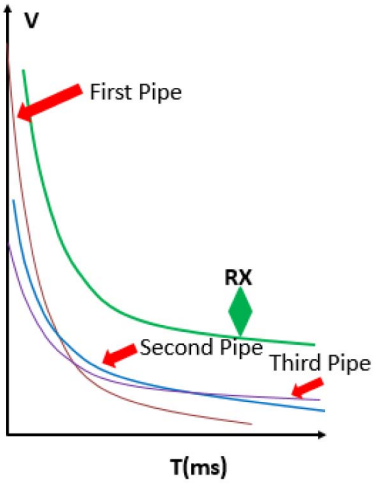

Figure 3b—Time domain voltage signal picked up by receiver

Our studies revealed that the RX signal not only includes the EC corresponding signal dB_{EC}/dt, but also unwanted interference related to extraneous tool movement, tubing remnant magnetization, and other noise. Consequentially, the deteriorated SNR of the RX signal for the outer pipes under the condition of multiple or large pipes makes thickness estimations inaccurate or even impossible. To physically analyze the problem, we can write the voltage detected by a receiver as Eq. 1.

$$S(t) \propto k_1 f_1(d\overline{B_{EC}}(t)/dt) + k_2 f_2([\bar{v}(t) + \sigma(\bar{v})] \times [\overline{B_r}(z) + \overline{B_{EC}}(t)]) + \sigma(e) \quad (1)$$

Where, $\overline{B_{EC}}(t)$ is the magnetic field generated by corresponding EC from pipes and $d\overline{B_{EC}}(t)/dt$ is the received RX signal; $v(t)$ is logging speed and $\sigma(\bar{v})$ is logging variation from extraneous tool motion; $\overline{B_r}(z)$ is the remnant magnetization; k_1 and k_2 are electronical gains, while f_1 and f_2 are tool transducer measurement functions, respectively; $\sigma(e)$ is the ePDT's electronic noise.

In the MTD tool, the signal dynamic range of *S(t)* for up to five pipes approximates 100dB to 120dB, the SNR for outer pipe can be in the range of −20dB to −40dB, which results their thickness estimation almost impossible. The noise mainly come from $\overline{B_r}(z)$ which is uncontrollable and randomly distributed on the tubing. Therefore, in order to decrease noise in the second term to the right of equation (1), we need to either reduce logging speed, extraneous tool motion, or minimize the output from of tool transfer function, k_2 and f_2.

Sensor Design and Tool Configuration

There are trade-offs among high charging power for high RX signal level versus transducer core saturation, total number of pipes detected versus proper logging resolution at acceptable logging speed, and extraneous tool motion versus SNR. The ePDT tool incorporates three transducers in different configurations and geometries as well as the carefully designed synthetic apertures, S, M, and L, respectively, as shown in Fig. 4a. The theoretical apertures of each transmitter are displayed on the right-side curves. To detect the inner pipe, the small transducer TX-S is operated to enable high SNR with high logging resolution. For the second and third pipes with OD less than 12", the medium transducer TX-M provides the optimally balanced measurements in resolution and SNR. The large transducer TX-L, delivers adequate SNR that is critical for producing high integrity measurements and analysis in the large and multiple tubulars environments.

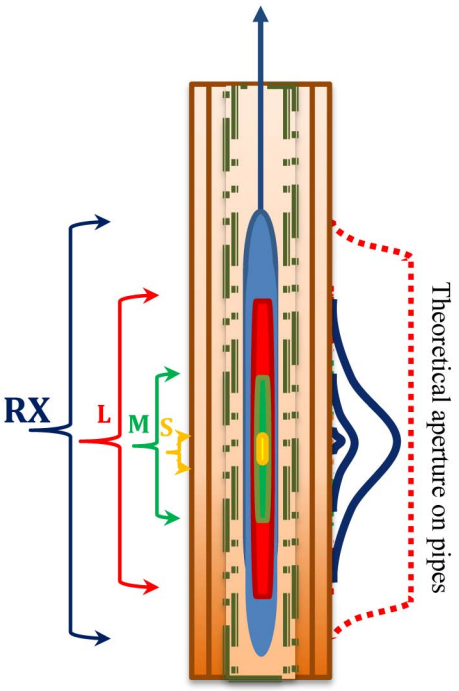

Figure 4a—ePDT sensor configurations

In addition, the variation of tubing EM parameters, conductivity and permeability, from joint-to joint largely impacts the RX signals for thickness estimations. Measurements of first tubular's EM properties are obtained from the TX-S, which provides the input for data correction. The correction method will be discussed in the next section.

Fig. 4b shows the COMSOL simulation results of sensor synthetic apertures, in which RX aperture is wider than TX apertures. During the logging acquisition, the RX signal is proportional to the convolution of RX aperture and EC spatial density distribution as shown in Fig. 4c. The RX aperture is associated with the motion of tool. The EC shape is initialized by the RX aperture and changing dynamically as a result of diffusion and damping in the pipes. The synthetic apertures design for TX and RX takes into account of sensor convolution, logging speed and tool motion jitters, as shown in Fig. 4b. Both simulation and lab tests show that the design can decrease uncertainty of f_2 in Eq. 1. This achieves better SNR by compensating extraneous tool motion and facilitates faster logging speed. In addition, the large RX spatial aperture functions as a narrow band-low-pass filter that reduces the $\overline{B_r}(z)$ in Eq. 1.

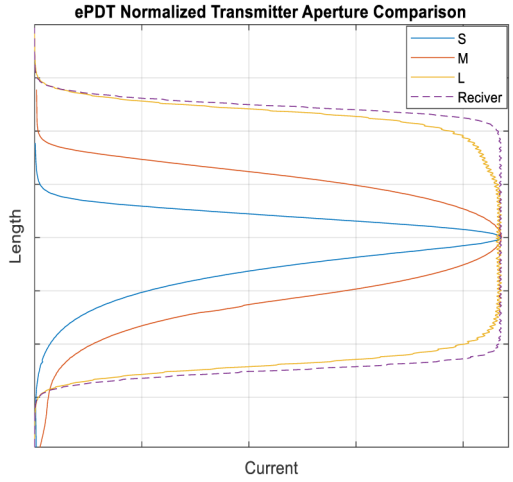

Figure 4b—Normalized transducer aperture on ePDT from COMSOL simulation

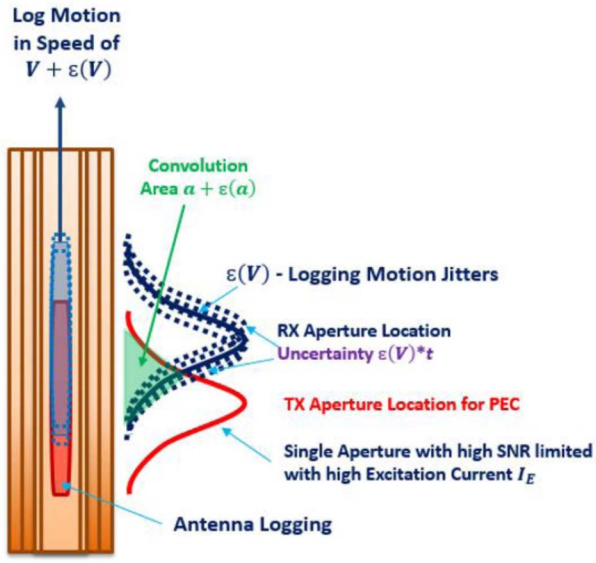

Figure 4c—Illustration of extraneous tool motion noise

Logging modes and speeds are optimized for any particular wellbore tubulars configuration. For instance, a small two-pipe configuration would only require TX-S and TX-M transducers activation with a corresponding logging speed of up to 25 FPM. For a large OD pipe with three or four pipes design, TX-S, TX-M and TX-L are activated and requires logging speed at 5 to 8 FPM.

Processing Algorithms

This section details the fast forward modeling that has been developed for simulating tool response, along with generating the inversion algorithm for each pipe's thickness calculation in any given wellbore tubulars configuration.

Forward Modeling

The forward modeling solves the electromotive force (EMF) induced on the receiving coil. Fig. 5a shows the physical model of ePDT. After the transmitting coil emits a pulse, eddy current is induced in the metallic pipes. According to Lenz's Law, the induced EMF will oppose the change in the magnetic flux generated by the induced eddy current

$$\varepsilon(t) = -\frac{d}{dt}\Psi(t)\,. \tag{2}$$

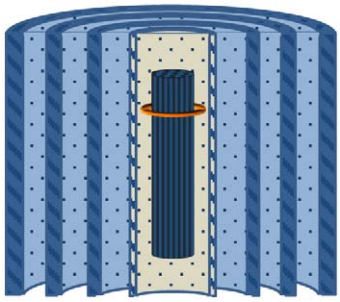

Figure 5a—Physical Model for ePDT

Instead of solving the magnetic field directly, the problem is converted into solving the vector potential in the diffusion equation in equation (4).

$$\nabla^2 \underline{A} - \mu\sigma\frac{\partial \underline{A}}{\partial t} = -\mu \underline{J_s}\,. \tag{3}$$

The equation is solved by applying Green's function method in frequency domain, then applying fast Fourier transform to get time domain decay curve.

Fig. 5b and Fig. 5c illustrates the match of both the radial and vertical boundary condition seen in. Eq. 4 is the electrical field continuation equation at vertical axis, Eq. 5 is the magnetic field continuation equation at the vertical axis, Eq. 6 is the electrical field continuation equation at the horizontal axis, and Eq. 7 is the magnetic field continuation equation at the horizontal axis. With all the equations and boundary condition at source and boundary, we are able to calculate the magnetic potential in the environment and therefore calculate the voltage of the receiver signal.

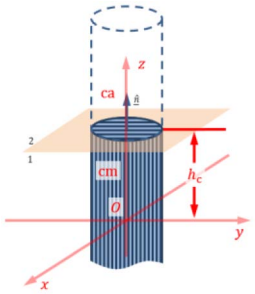

Figure 5b—Vertical boundary conditions

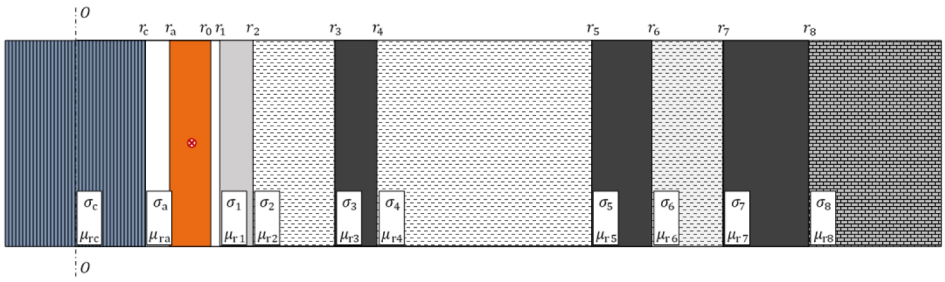

Figure 5c—Horizontal boundary conditions

$$G^{(\mathrm{ca})}\left(r,\ h_c; r', z'\right) = G^{(\mathrm{cm})}(r, h_c; r', z') \tag{4}$$

$$\frac{1}{\mu_{\mathrm{ca}}}\frac{\partial G^{(\mathrm{ca})}(r,h_{\mathrm{c}};r',z\prime)}{\partial z}=\frac{1}{\mu_{\mathrm{cm}}}\frac{\partial G^{(\mathrm{cm})}(r,h_{\mathrm{c}};r',z\prime)}{\partial z} \tag{5}$$

$$G^{(\ell-1)}(r_\ell,z;r',z')=G^{(\ell)}(r_\ell,z;r',z') \tag{6}$$

$$\frac{1}{\mu_{\ell-1}}\left(\frac{G^{(\ell-1)}(r_\ell,z;r',z')}{r_\ell}+\frac{\partial G^{(\ell-1)}(r_\ell,z;r',z')}{\partial r}\right)= \frac{1}{\mu_\ell}\left(\frac{G^{(\ell)}(r_\ell,z;r',z\prime)}{r_\ell}+\frac{\partial G^{(\ell)}(r_\ell,z;r',z\prime)}{\partial r}\right)+\delta_{r_\ell r\prime}\delta(z-z')\,. \tag{7}$$

The forward modeling is validated by COMSOL FEM simulation for the typical size and thickness of a four-pipe combination as illustrated in Fig. 6.

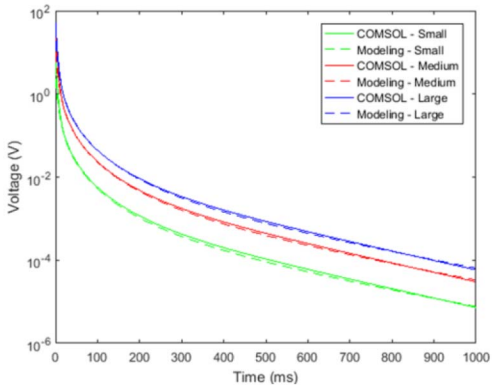

Figure 6—Forward modeling results versus COMSOL modeling, the TX-S, TX-M and TX-L transducers exhibit an excellent match between COMSOL and forward modeling

Thickness Calculation

With the fast forward modeling algorithm, the model based inversion calculates the thickness of each pipes. Fig. 7 provides the workflow of the inversion. The input of σ and μ are from the dataset of the small transducer measurement. With input parameters from well schematic, by minimizing the cost function through optimization kernel, the thickness of each pipe can be calculated.

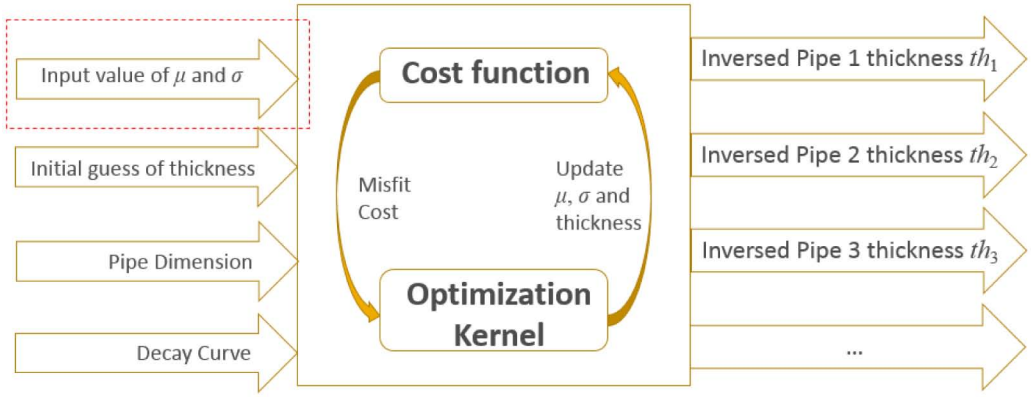

Figure 7—Flow diagram of inversion, the red box indicates the σ and μ is calculated from tubing EM parameter inversion via TX-S data

The cost function is defined in Eq. 8:

$$Cost(x)=\frac{1}{2m}\sum_{i=1}^{m}\|W_i*\{log(x_i)-log(x_{norm})\}\|^2+|W_x*(log(x)-log(x_{norm}))| \tag{8}$$

Where

m is total channels measured by tool, which includes the eddy current signal from each pipe;

x_i is the voltage measured by tool; and x_{norm} is the voltage calculated by forward modeling;

W_i is the weight function for each measurement channel, where W_x is the weight for channel regularization.

Since the voltage on receiver coil decays logarithmically in each measurement channel, to differentiate voltage logarithmically will result in similar entropy for each channel, and thickness calculation more accurate.

ePDT Lab Validation

Both stationary and motion test have been performed to validate the tool performance. This section provides the results for these validations.

Sensor Verification

Fig. 8a below shows the stationary sensor testing in lab with four pipes, first pipe OD 5.5", thickness 0.275", second pipe OD 9-5/8", thickness 0.352", third pipe OD 13-3/8", thickness 0.33", and fourth OD pipe 20", thickness 0.375". Fig. 8b shows the tool measurement results that exhibit a good match compared to forward modeling. The slight difference in late channel response can be attributed to unknown EM parameter of pipes.

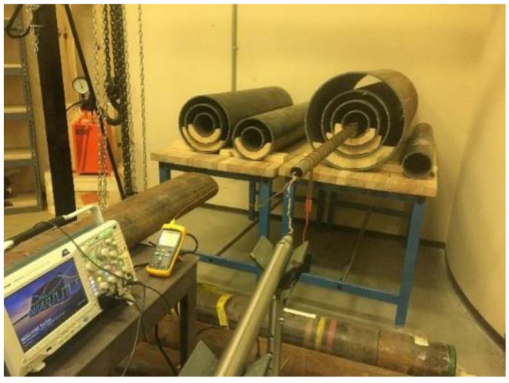

Figure 8a—Lab setup of four pipes nested concentrically

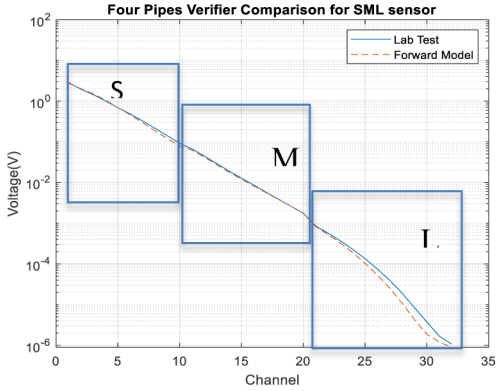

Figure 8b—Four pipes result comparison: tool data and forward modeling decay curves match very well

Tool motion verification

Fig. 9a shows the tool is logged at 7 FPM inside a three-pipe configuration, a 21" OD × 6" long collar is placed outside the 20" pipe. Fig. 9b depicts the schematic of this test setup. Fig. 9c illustrates the VDL during

the test, in which the 21" collar is clearly visible on VDL and indicates as a 20% increase in calculated thickness.

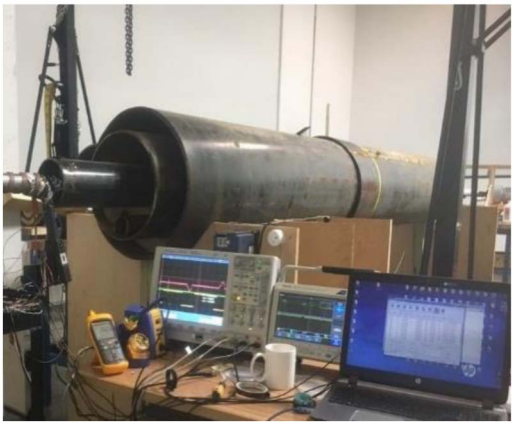

Figure 9a—Lab test of tool moving inside three pipes with 21″ collar outside

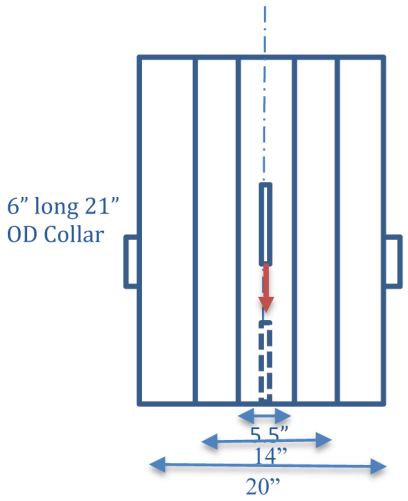

Figure 9b—Pipe configurations

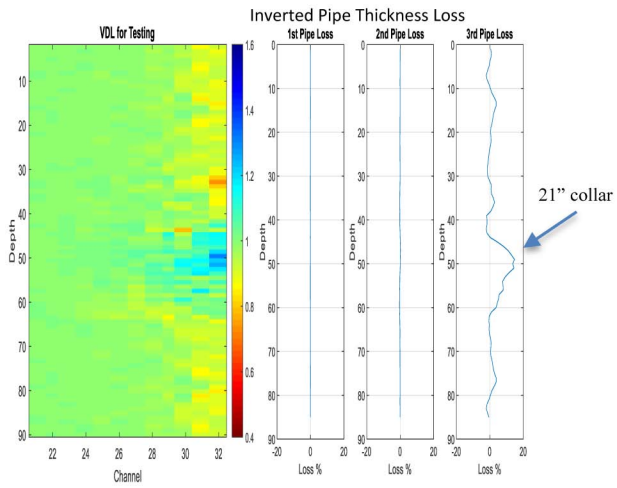

Figure 9c—VDL of test in 7 FPM, at depth 45-55, we can clearly see the 21″ collar in blue color

Field Test Examples

This section describes the results of two field log examples from Texas Gulf Coast cavern storage wells. One case has four pipes, with a largest pipe OD of 30", and a logging speed of 7-9 FPM. The other case has two pipes with fast logging speed of 25 FPM.

Case #1 - Three to Four Pipes

Fig. 10 displays the log of the three large size pipes. The size and weight of each pipe are stated on the top right corner of the figure. Collars from all three pipes are clearly identified on the VDL displays. Severe damage is indicated to the third pipe in several localized areas over a 125ft interval, the metal loss ranges from 27% to 40%.

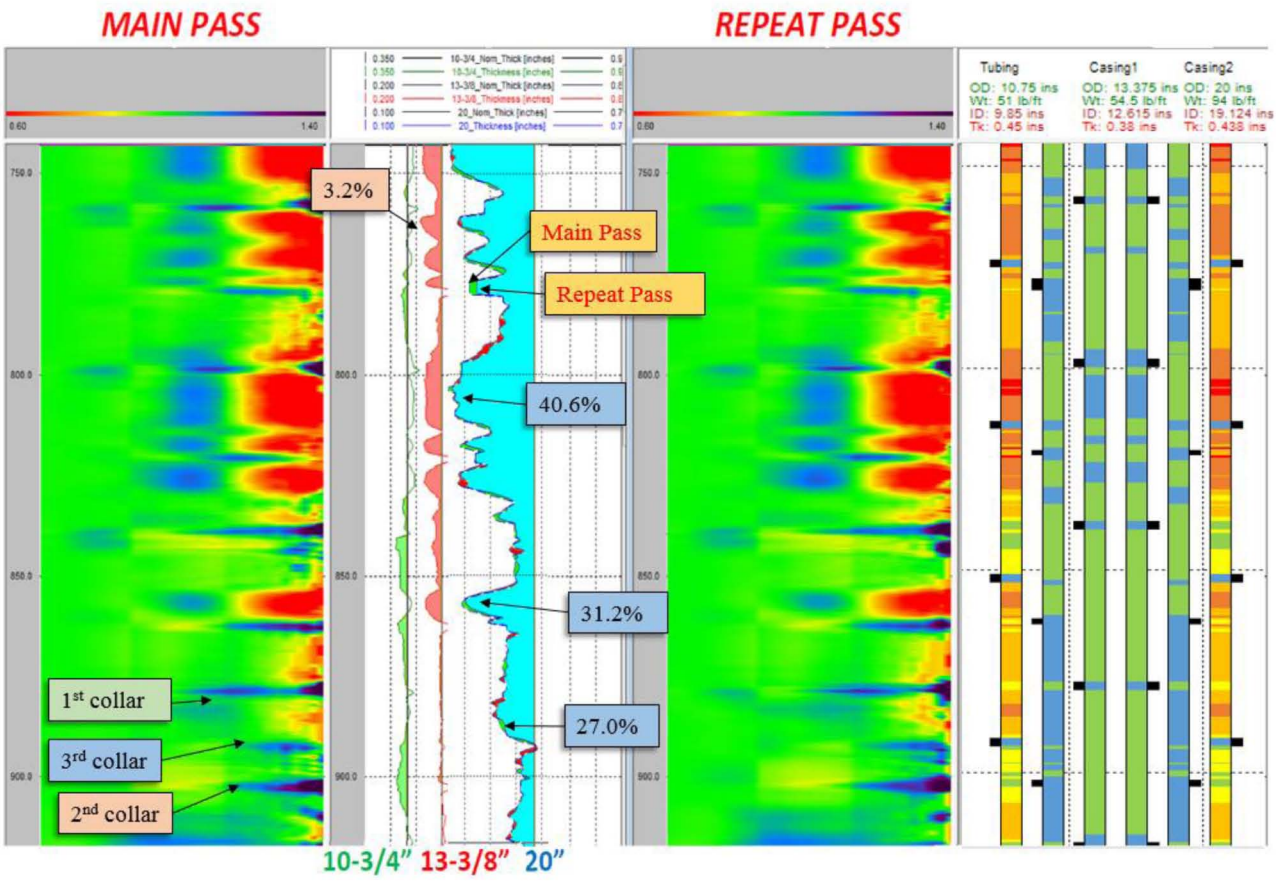

Figure 10—Field test data logged in three pipes, massive corrosion of the third pipe is detected

Comparison of main pass versus repeat pass demonstrates the excellent repeatability of data in both highly and slightly corroded 20" casing. The under 2% variance between passes may be attributable to comes from logging motion noise, which has insignificant influence on the analysis.

Fig. 11 displays the RAW data from the same well in different depth just above and below the 30" casing shoe. The casing shoe is clearly identified at around 350ft. Above the shoe joint, welded joints were used, resulting in negligible signal change at the 30" connections. From the raw data in the middle figure, compare curves from 300-350ft to 400-450ft, we can clearly see the base lines are shifted for late channels ADEC26-31, which indicates that the additional signal detected by the receiver is attributable to the 30" casing. Under ideal conditions, this could allow quantitative evaluation of even the 30" pipe.

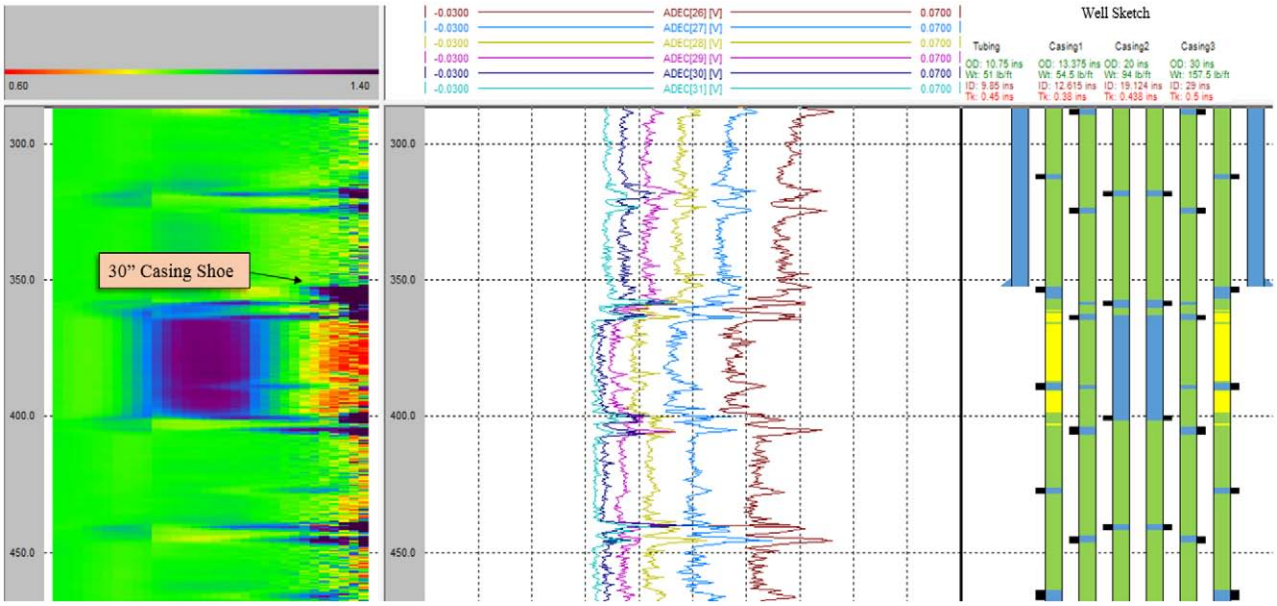

Figure 11—Field test data logged in three and four pipes, the 30" casing shoe is clearly detected

Case #2 - Fast Logging Test in Two String Configuration

Fig. 12 shows the analysis of a 4.5" OD + 7-5/8" OD configuration, the logging speed is 25 FPM. The VDL shows highly integrity log data and excellent SNR. The 8.4% corrosion on the outer pipe is picked up from this log. It demonstrates that ePDT works well at high logging speed when there's one or two pipes shown.

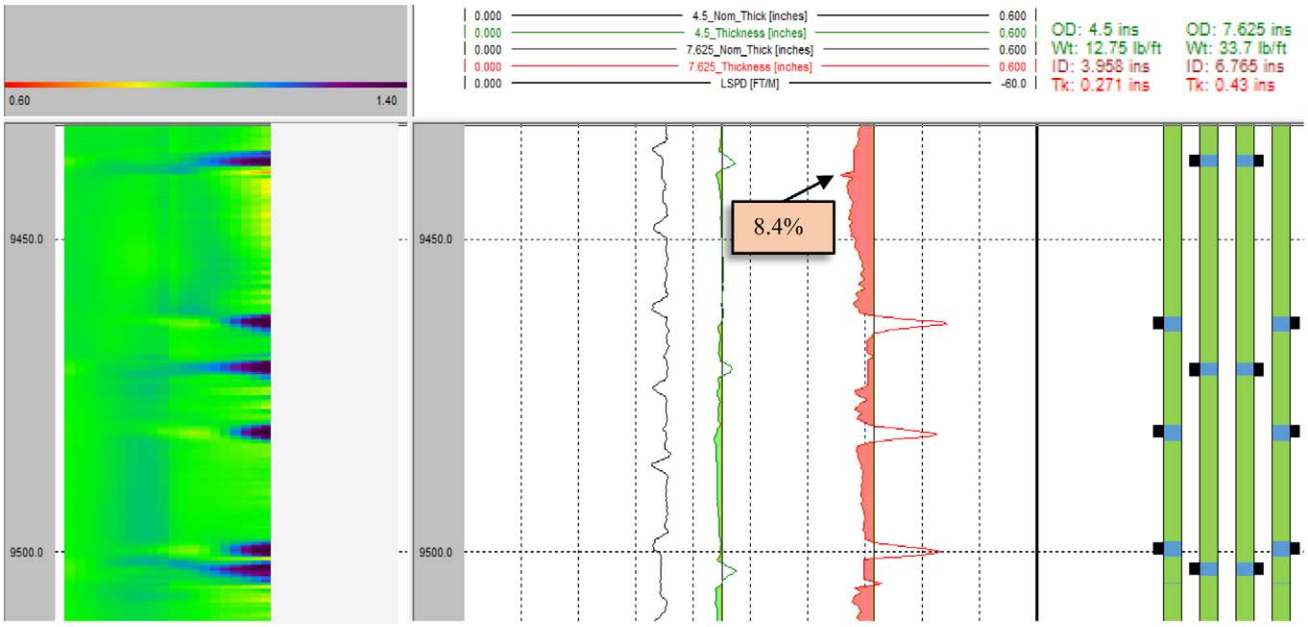

Figure 12—Field test in two pipes at logging speed of 25 FPM

Conclusions

This paper presented the information about the field-worthy 2" OD ePDT instrument with its innovative sensor, which provides a synthetic TX-RX aperture in different measurement configurations. This innovative design permits high SNR for large pipe evaluation, optimal vertical resolution for inner pipe analysis, and increased logging speed for optimized acquisition efficiency.

Field tests performed by the tool demonstrated that high integrity measurements and analysis can be produced for 20" OD pipe in the presence of 13-3/8" and 10-3/4" pipes, along with inferring potential for evaluating a 30" pipe present in the same tubulars configuration.

In summary, ePDT can deliver the unique well integrity evaluation solution over a wide range of metallic tubulars sizes and configurations in an efficient and effective way.

Acknowledgements

The authors would like to thank the cavern storage well operators who have supported the field trials of the ePDT tool and have granted permission to display their data in this publication.

References

Yanxiang, Y., 2016. Fractal magnetic sensor array using mega matrix decomposition method for downhole application, US Patent No. 10,061,050.

Yanxiang, Y., 2016. Method and apparatus for synthetic magnetic sensor aperture using eddy current time transient measurement for downhole applications, US Patent No. 10,082,593.

Rourke, M., Li, Y., 2013. Multi-Tubular Corrosion Inspection Using a Pulsed Eddy Current Logging Tool. International Petroleum Technology Conference. IPTC-16645-MS.

Rourke, M., Jin, Y., 2014. Algorithm Development and Case Study for A 1-11/16" Pulsed Eddy Current Casing Inspection Tool. Society of Petrophysicists and Well-Log Analysts.

Martin, L. E. S., Fouda, A. E., 2017. New High-Definition Frequency Tool for Tubing and Multiple Casing Corrosion Detection. Society of Petroleum Engineers. SPE-188932-MS.

Omar, S., Omeragic, D. 2018. Use of apparent thickness for preprocessing of low-frequency electromagnetic data in inversion-based multibarrier evaluation workflow. *AIP Publishing*. Vol. **1949**, No. 1, p. 020017.